DEVELOPING OF A NEW COMPREHENSIVE SPARK IGNITION ENGINES CODE FOR HEAT LOSS ANALYSIS WITHIN COMBUSTION CHAMBER WALLS

by

Shahram KHALILARYA and Mohammad JAVADZADEH *

Department of Mechanical Engineering, Urmia University, Urmia, Iran

Original scientific paper
UDC: 621.434:519.876.2/.5
DOI: 10.2298/TSCI10041013K

The objective of this work is to develop the existing a zero-dimensional model named ODES to provide detailed insights into the internal process of the modern high speed spark ignition engines. Therefore, it has been concentrated on the development of new sub models for incorporation in an extended form of ODES, as follows:
– the existing semi-empirical combustion model has been replaced by a new comprehensive model, which is based on the turbulent flame speed in the combustion chamber.
– the existing three wall heat transfer model has been replaced by a new one in which, the combustion chamber is divided in to three zones including cylinder head, cylinder wall, and piston head. The steady-state heat transfer equation is solved through finite difference method with replaced boundary and initial conditions. The results gave the temperature distribution of combustion chamber walls. The rate of heat losses from combustion chamber to the coolant is calculated by using the mean temperature of each part. The code has been extensively validated with respect to performance and heat transfer against experimental results obtained on XU7JP spark ignition engine with two kinds of fuel, gasoline and compresed natural gas and gave good agreement with available experimental.

Key words: *zero dimensional, turbulent flame, combustion chamber, finite difference*

Introduction

The development of modern internal combustion engines is aimed at very high levels of effective power and fuel efficiency at extremely low exhaust emissions. To reduce time and cost for engine development on the test bench, reliable pre-optimization of the thermodynamic working cycle by simulation is necessary. Universally valid model formulations, which are primarily based on physical laws, are needed for the description of combustion, heat losses, and emission formation.

* Corresponding author; e-mail: mjavadzadeh2007@gmail.com

Combustion is the most important process taking place in spark ignition (SI) engines, through which chemical energy of fuel is converted into sensible internal energy of the cylinder charge. In the past, different approaches for combustion in SI engines were developed [1-7]. During this process, a turbulent flame, which is a roughly spherical in shape, propagates across the combustion chamber and burns the premixed fuel-air mixture [8, 9]. Therefore, combustion can be considered as a turbulent flame propagation process. Details of the flame propagation have substantial effect on combustion, and therefore on energy conversion process and heat losses [10].

Thomas [11] studied about flame development in SI engines. He discussed that reduced knock can lead to operation with higher compression ratios and with leaner mixtures. Thus, higher efficiency, higher power output, and more stable engine operation could be obtained. Lucas [12] and Poulos [13] studied on the effect of combustion chamber shape on the rate of combustion in a SI engine in two ways. The first is to generate a more turbulent charge motion via the use of intake flow restrictions or combustion chambers with large squish regions. The second is to increase the flame front area by minimizing the contacts between the flame and chamber walls. This requires using a more compact combustion chamber and moving the spark plug electrodes toward the chamber center. It is obvious that such methods necessitate some modifications on intake system and combustion chamber design. The combustion processes in the two-dimensional flow field of a spark ignition engine were calculated numerically by Basso [14], in order to examine the effect of combustion chamber configuration on the thermal efficiency.

A two-dimensional combustion process in a SI engine was calculated numerically by Hano *et al.* [15] using k-ε turbulence model, flame kernel ignition model, and an irreversible reaction model to obtain a better understanding of the spatial and temporal distributions of the flow and combustion.

Beside combustion models, an accurate heat transfer model can be used to predict the engine heat transfer rate which is very important for thermal load analysis, combustion performance and engine components such as pistons, valves, and rings life time.

During recent years, the interest in the heat transfer phenomena in reciprocating internal combustion engines has been widely intensified because of their major importance among other aspects on successful thermodynamic cycle simulation [16-19]. Oguri [20] studied on the coefficient of heat transfer between gases and cylinder walls of the SI engines. He used Eichelberg's method to predict the heat transfer rate in SI engines. His predicted results agreed with the experimental results for expansion stroke but not for the compression stroke. This might be because the model was established for diesel engines and was not suitable for SI engines. Alkidas and his co-workers [21, 22] measured instantaneous heat flux in the combustion chamber of SI engines. They found that heat fluxes could be affected by the engine speed and air-fuel ratio. Shayler [23] determined the heat transfer from the combustion chambers of SI engines in two ways. In the first method he used the first thermodynamic law, but the results were not satisfactory. In the second method the heat transfer rates were calculated based on Woschni's, Annand's, and Eichelberg's experimental models. It was found that Eichelberg's method could predict closest results to the experimental data.

Short calculation time is important for the optimization of the large and still increasing number of hardware and operating parameters, which leads directly to zero-dimensional simulation models.

In this paper, the general strategy for the development of combustion models is based on zero-dimensional formulations, which means that, compared to three-dimensional computational fluid dynamics (CFD) codes, there are advantages regarding calculation time, easy handling, and required number of model constants. On the other hand, there are limitations such as less detailed description of mixture preparation and combustion process and the lacking capability to take into account three-dimensional effects due to the geometry of the combustion chamber. In the new heat transfer model, the combustion chamber is divided into three zones including cylinder head, cylinder wall, and piston head. The steady-state heat conduction equation is solved by using the alternative direction implicit (ADI) method with replaced boundary and initial conditions. The results gave the temperature distribution of combustion chamber walls. By using the mean temperature of each part and the coolant temperature in the convective heat transfer equation, the rate of heat loss from combustion chamber walls to the coolant is calculated.

ODES model

The existing Fortran 77 code named ODES (Otto-Diesel-Engine-Simulation) developed at the University of Bath by Wallace and co-workers in 1993 [24]. Then extended by Khalilarya for diesel engine simulation in 2002 [25]. In the present work the existing heat release model is replaced by a new comprehensive one, which is based on the turbulent flame speed in the combustion chamber and heat transfer model replaced by a new one which is based on finite difference methods to simulate SI engines heat release and heat losses. This code is a thermodynamic model which uses filling and empting methods, mass and energy conversion laws. The engine is introduced through thermodynamic control volumes, flow restrictions and shafts to the model. Figure 1 outlines the ideas behind and structure within the model [26].

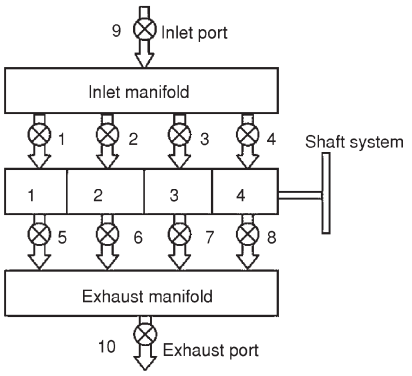

Figure 1. Control volumes and flow restrictions and shaft system for engine

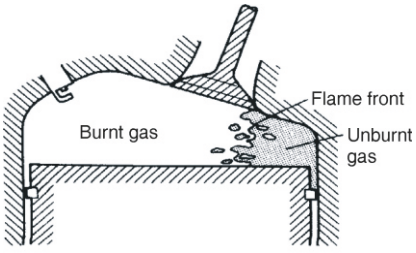

Figure 2. Two zones in combustion chamber of SI engines

The governing equations of this model have been derived by applying the first law of thermodynamic on cylinder charge, which are time-dependent, first-order ordinary differential equations. In this model, cylinder charge is considered as an ideal gas mixture. During intake and compression stroke, cylinder content is regarded as a non-reacting ideal gas mixture of air, fuel vapor, and residual burned gases. Throughout the combustion process, the cylinder is considered to consist of two thermodynamic regions which are separated by a thin spherical flame front, the unburned gas region and the burned gas region (*e. g.* fig. 2) [27].

During expansion, only burned gases are assumed to exist in the cylinder. Temperature, pressure, mass amount, and other gas properties in every crank angle will be available for each control volume by calculating mass perpetuity, energy and gas component conversion eqs. (1)-(3).

$$\frac{\partial T}{\mathrm{d}t} \quad \frac{1}{m\dfrac{\partial U}{\partial t}} \quad \frac{\mathrm{d}Q_{\mathrm{w}}}{\mathrm{d}t} \quad \frac{\mathrm{d}Q_{\mathrm{f}}}{\mathrm{d}t} \quad h_{\mathrm{i}}\frac{\mathrm{d}m_{\mathrm{i}}}{\mathrm{d}t} \quad h_{\mathrm{e}}\frac{\mathrm{d}m_{\mathrm{e}}}{\mathrm{d}t} \quad m\frac{\partial U}{\partial \lambda}\frac{\mathrm{d}\lambda}{\mathrm{d}t} \quad \frac{m\mathrm{R}T}{V}\frac{\mathrm{d}V}{\mathrm{d}t} \quad U\frac{\mathrm{d}m}{\mathrm{d}t} \tag{1}$$

$$\frac{\mathrm{d}m}{\mathrm{d}t} \quad \frac{\mathrm{d}m_{\mathrm{i}}}{\mathrm{d}t} \quad \frac{\mathrm{d}m_{\mathrm{e}}}{\mathrm{d}t} \quad \frac{\mathrm{d}m_{\mathrm{f}}}{\mathrm{d}t} \tag{2}$$

$$\frac{\mathrm{d}\lambda}{\mathrm{d}t} \quad \frac{1 \quad \lambda}{m}\frac{\mathrm{d}m_{\mathrm{f}}}{\mathrm{d}t} \quad \frac{\mathrm{d}m_{\mathrm{i}}}{\mathrm{d}t}\frac{\lambda_{\mathrm{i}} \quad \lambda}{1 \quad \lambda} \tag{3}$$

By solving these equations through initial values for T, m, and λ numerical integration will start. This code uses a prediction-corrector method which calculates T, m, and λ step by step in each cycle. By using eq. (4) the pressure in each crank angle is obtained and through eq. (5) the power is calculated for each time step:

$$PV = m\mathrm{R}T \tag{4}$$

$$\frac{\mathrm{d}w}{\mathrm{d}t} \quad \frac{P\mathrm{d}V}{\mathrm{d}t} \tag{5}$$

Through filling and empting control volumes the main assumptions that have been considered in developing this model are mentioned as [28]:

– quasi-Steady: in this case the above equations are solved in separate time steps. So variables are constant in every time step. Beside, the calculation accuracy will increase by using small time steps,
– semi ideal gas: specific heat coefficient in constant pressure and constant volume varies by temperature but follows from gas status equation,
– cylinder contents during induction, compression and expansion processes are assumed to be a homogeneous gas mixture of air, fuel vapor and products of combustion,
– during combustion process, the cylinder contents are considered to consist of two zones, burned and unburned gases; each zone has uniform local thermodynamic properties, and
– thermodynamic properties of gases are calculated using ideal gas laws with temperature dependent specific heats; pressure inside the cylinder is assumed to be uniform and varies with the crank angle; the gas motion inside the cylinder (created by small pressure gradients due to piston motion) is neglected; for each control volume different heat transfer and heat release models can be used.

Heat transfer model

The heat transfer rate, from gas to the combustion chamber wall is determined by forced convection equation [29, 30] and can be expressed as:

$$Q_{\mathrm{w}} = f_{\mathrm{s}}h_{\mathrm{c}}A(T_{\mathrm{g}} - T_{\mathrm{w}}) \tag{6}$$

The heat transfer process between two zones depends on the shape and the area of the flame front. Such a complicated process is difficult to be modeled. Due to the crucial role of heat transfer in the design of engines, all computer programs for simulation of internal combustion engines include a heat transfer model. Many models have been proposed for the heat transfer coefficient, assuming that the heat flux is the same for the entire heat transfer surface.

Nusselt's [31] model was the first engine heat transfer model based on a spherical bomb. Originally it was used to predict the steady-state heat flux. It can also be used to predict the instantaneous heat flux. Annand [32] proposed a heat transfer model based on the steady-state turbulent convection. Eichelberg's [33] model has been widely used to study the heat transfer in large-scale two-stroke and four-stroke diesel engines.

In this study in order to provide a simple heat transfer model, but yet accurate enough, for the engine simulation, a heat transfer coefficient using the Woschni [34] correlation is used for the fluid flow and combustion modeling of fuel mixture which determines the gas temperature and local heat fluxes in the chamber walls, eqs. (7) and (8). To simplify the case, a reasonable assumption of flow over a flat plate is used:

$$h_c = CD^{m-1}P^m W^m T^{(0.75-1.62\,m)} \tag{7}$$

Woschni's correlation, with the exponent in eq. (7) with $m = 0.8$ and $C = 3.26$ is summarized in eq. (8) [35]:

$$h_c = 3.26D^{-0.2}P^{0.8}W^{0.8}T^{-0.546} \tag{8}$$

Heat release model

Combustion is modeled as a turbulent flame entrainment process. This model has been described by Blizard *et al*. [36] at first. Further refined by Tabaczynski [37] and Poulos [38]. The rate of propagation of ignition sites is given by the sum of turbulent intensity and laminar flame speed [39].

In the present heat release model, the flame propagation type is based on the cylinder flow field. It is assumed that the charge is first engulfed by the flame front along highly dissipative regions or vortex tubes with the turbulent flame velocity and then burns across the spacing characterized by a flame factor, unburned gas density, and the laminar flame velocity. Equation (9) shows the heat release calculation method:

$$\frac{dQ_f}{dt} \quad ffA_f\rho_u S_l q_{vs.} \tag{9}$$

A cubic spline function is used to give a smooth curve-fit for the flame front area and fuel concentration at the different cross-sections. Thus, the model can simulate the effect of chamber shape and fuel distribution. The model also gives a description of the minimum SI energy and flame pattern, based on the cylinder flow field. Equations (10)-(15) show the relations used to calculate laminar flame speed [40]:

$$ff \quad 1 \quad \frac{S_t}{S_l} \tag{10}$$

$$S_l \quad S_u \quad \frac{\rho_b}{\rho_u} \tag{11}$$

$$S_u \quad S_{u,0} \quad \frac{T_u}{T_0}^{\alpha} \quad \frac{P}{P_0}^{\beta} \tag{12}$$

$$S_{u,0} = B_m + B_\phi(\phi - \phi_m)^2 \tag{13}$$

$$\beta = -0.16 + 0.22(\phi - 1) \tag{14}$$

$$\alpha = 2.218 - 0.8(\phi - 1) \tag{15}$$

Equations (16)-(18) indicate the relation between laminar and turbulent flame speed, in which a specific turbulent Reynolds function is used:

$$S_t = fsr \cdot S_l \tag{16}$$

$$fsr \quad 0.2625 \ 10^{-4} \mathrm{Re}_{turbu}^2 \quad 3.95 \ 10^{-2} \mathrm{Re}_{turbu}^2 \quad 1 \tag{17}$$

$$\mathrm{Re}_{turbu} \quad \frac{u \, l_i}{\nu} \tag{18}$$

In the present developed ODES code, the turbulent intensity is firstly assumed 60 percent of engine speed and then through the program is corrected by unburned gas mixture specific density as eq. (19):

$$u \quad 0.6 S_p \left(\frac{\rho_u(\theta \quad \Delta\theta)}{\rho_u(\theta)} \right)^{0.33} \tag{19}$$

Table 1. Parameters values

Fuel	ϕ_m	B_m	B_ϕ
Methanol	1.11	36.9	–141
Propane	1.08	34.2	–139
Isooctane	1.13	26.3	–85
Gasoline	1.21	30.5	–55

Within the restrictions of homogeneous and isotropic turbulence, an energy budget can be used to relate l_i and l_m as in eqs. (20) and (21):

$$\varepsilon \quad \frac{u^3}{l_i} \quad \frac{15\nu u^2}{l_m^2} \tag{20}$$

$$l_i \quad l_m \sqrt{\frac{\mathrm{Re}_{turbu}}{15}} \tag{21}$$

Values of constant parameters are defined in tab. 1 [40].

Heat losses model

Satisfactory engine heat loss is required for a number of important reasons, including emissions, knock, and material temperature limits. Since the combustion process in an internal combustion engine is not continuous as in the case for an external combustion engine, the components temperatures are much less than the peak combustion temperatures. However, the temperatures of certain critical areas need to be kept below material design limits.

The heat transfer rate in an engine is dependent on the coolant temperature and the engine size, among other variables. There are complex interactions between various operational parameters. For example, as the temperature of the engine coolant decreases, the heat loss to the coolant will increase, and the combustion temperature will decrease. This will cause a decrease in the combustion efficiency and engine power. It will also cause an increase in the thermal stresses in the cylinder sleeve, and in the size of the radiator needed.

For calculating heat loss rate from running engine to the surrounding coolant the convection heat transfer equation is used, *e. g*. eqs. (22)-(24):

$$Q_{\text{head}} = f_s h_{\text{water}} A_{\text{head}} (T_{\text{water}} - T_{\text{w, head}}) \tag{22}$$

$$Q_{\text{piston}} = f_s h_{\text{oil}} A_{\text{piston}} (T_{\text{oil}} - T_{\text{w, piston}}) \tag{23}$$

$$Q_{\text{liner}} = f_s h_{\text{water}} A_{\text{liner}} (T_{\text{water}} - T_{\text{w, liner)}} \tag{24}$$

The approach to determine the combustion chamber temperature such as temperature of piston crown ($T_{\text{w, piston}}$), cylinder head ($T_{\text{w, head}}$), and cylinder wall ($T_{\text{w, liner}}$) is deduced from the energy conservation law.

To obtain the temperature distribution in engine components, a 2-D axisymmetric finite-difference heat conduction model, *e. g.* eq. (25), is developed [41]. In the engine geometry, some boundary points have specified temperatures and others have specified heat fluxes. Wall heat flux boundary conditions are obtained from ODES new combustion model. To calculate steady-state surface temperature distribution, finite difference code is run in an iterative sequence. First, a modified version of ODES, is run to obtain heat flux on chamber walls, next, the finite difference code generates a surface temperature profile, based on the heat flux data from ODES, which will be used to calculate surfaces temperature distributions. Using this method, mean temperature for chamber walls and heat losses to the coolant through each part are determined:

$$\frac{\partial T}{\partial t} \quad \alpha \quad \frac{\partial^2 T}{\partial x^2} \quad \frac{\partial^2 T}{\partial y^2} \tag{25}$$

As the boundary condition, the temperatures on the outer surface of the cylinder wall, cylinder head, and piston head were treated from convection between surfaces and the coolant. Temperature of the coolants such as oil and water are assumed to be constant. This is reasonable because the variation of the temperature on these coolants is much smaller than that on the inner surfaces of the combustion chamber. The boundary condition on the inner gas-side surface of the combustion chamber was a specified heat flux, which was obtained through the cycle simulation process by the ODES.

The numerical method used here to calculate the temperature distribution on the combustion chamber is the ADI method which is an accurate one, *e. g.* eqs. (26) and (27):

$$\frac{T_{ij}^{n\ 1/2} \quad T_{ij}^{n}}{\frac{\Delta t}{2}} \quad \alpha \quad \frac{T_{i\ 1,j}^{n\ 1/2} \quad 2T_{ij}^{n\ 1/2} \quad T_{i\ 1,j}^{n\ 1/2}}{\Delta x^2} \quad \frac{T_{i,j\ 1}^{n} \quad 2T_{ij}^{n} \quad T_{i,j\ 1}^{n}}{\Delta y^2} \tag{26}$$

$$\frac{T_{ij}^{n\ 1} \quad T_{ij}^{n\ 1/2}}{\frac{\Delta t}{2}} \quad \alpha \quad \frac{T_{i\ 1,j}^{n\ 1} \quad 2T_{ij}^{n\ 1} \quad T_{i\ 1,j}^{n\ 1}}{\Delta x^2} \quad \frac{T_{i,j\ 1}^{n\ 1/2} \quad 2T_{ij}^{n\ 1/2} \quad T_{i,j\ 1}^{n\ 1/2}}{\Delta y^2} \tag{27}$$

By calculating temperature distribution in combustion chamber through ADI method a mean temperature is used for each part in eqs. (22)-(24).

Equations (28) and (29) are used to calculate the local heat transfer coefficient for the cooling fluid [42]:

$$h \quad \frac{\text{Nu}k}{D} \tag{28}$$

$$\mathrm{Nu} \quad 0.3 \quad \frac{0.62\sqrt{\mathrm{Re}}\sqrt[3]{\mathrm{Pr}}}{\sqrt[4]{1 \quad \frac{0.4}{\sqrt[3]{\mathrm{Pr}^{2}}}}} \quad 1 \quad \sqrt{\frac{\mathrm{Re}}{282000}} \tag{29}$$

Finally, all new sub models have been fully integrated into a new comprehensive simulation package designated ODES2.

Table 2. Engine specifications

Engine model	XU7JP
Engine type	Four stroke, water cooled
Cylinder bore	83 mm
Stroke	81.4 mm
Connecting rod length	150.15 mm
Compression ratio	9.25:1
Engine speed	2500-5500 rpm
Fuel system	Gasoline-CNG

Model validation

The experimental results were carried out on a four cylinder, water-cooled, four stroke SI engine. The engine specifications are shown in tab. 2 [43].

Results and discussions

Temperature distributions

The validity of the present simulation model was evaluated by comparing its results with the experimental results at the same operating conditions and parameters.

According to the engine specifications, a finite difference method to calculate temperature distribution in this engine was set up. Figure 3 shows the grids and boundary conditions of the model for the fine grid option.

Figures 4-6 show the temperature distributions on cylinder wall, cylinder head, and piston head, respectively.

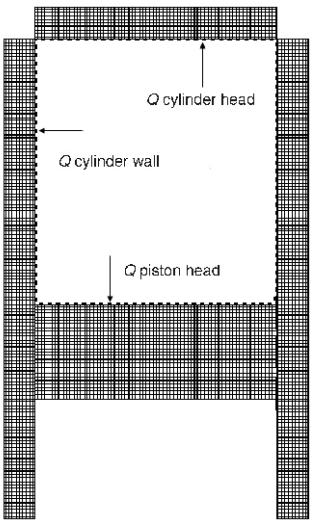

Figure 3. Numerical mesh of XU7JP SI engine

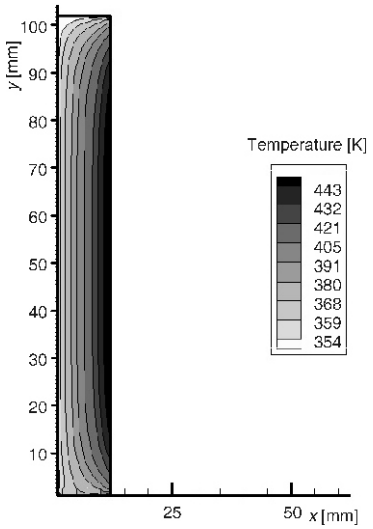

Figure 4. Temperature distribution for the cylinder wall

Engine performance parameters

The accuracy of the new combustion model is verified by comparing the predicted results with those given in ref. [43]. Figures 7-9 compare the predicted torque, power and brake specific fuel consumption for gasoline fuel in 2500-5500 rpm engine speeds which show the reasonable agreement between them.

In this study, the fuel type also has been investi-

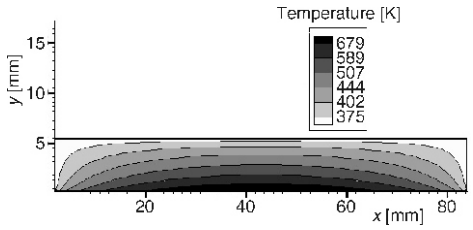

Figure 5. Temperature distribution for cylinder head

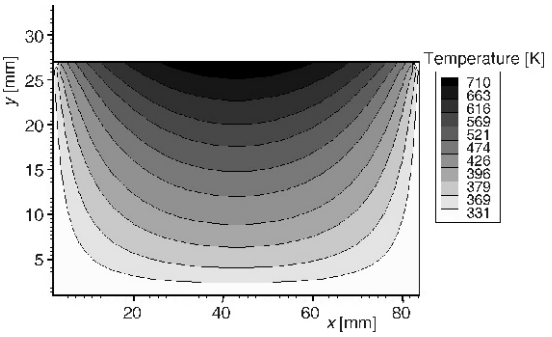

Figure 6. Temperature distribution for piston

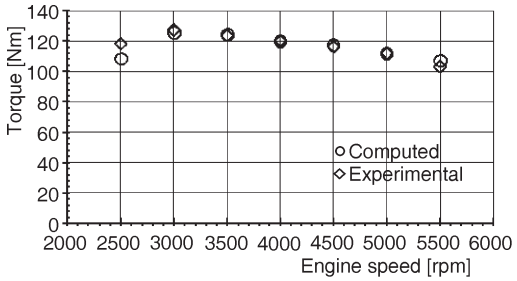

Figure 7. Engine torque for gasoline fuel

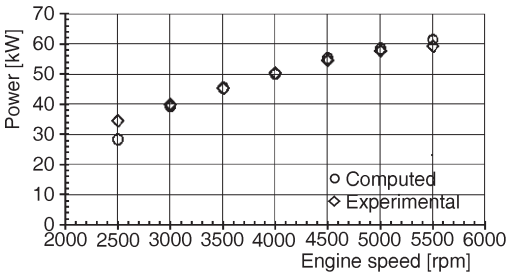

Figure 8. Engine power for gasoline fuel

gated in addition to the effect of engine variables. Since methane is the major component of natural gas, thus, methane is used as an alternative fuel for this investigation. Therefore, the gasoline has been replaced with methane and the effect of various parameters has been studied. According to the results, the torque and power reduced for the engine fueled with compresed natural gas (CNG) without any special change in the characteristics. Engine torque and power compared to experimental data for 2500-5500 rpm speeds are shown in figs. 10 and 11, for CNG fuel, respectively.

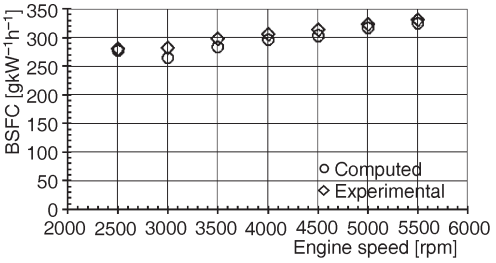

Figure 9. Engine brake specific fuel consumption for gasoline fuel

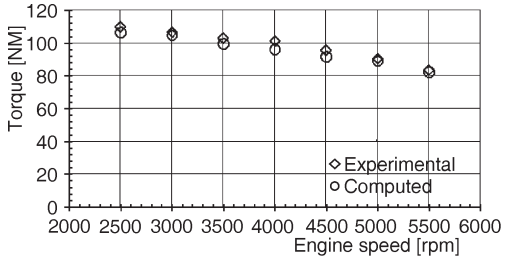

Figure 10. Engine torque for CNG fuel

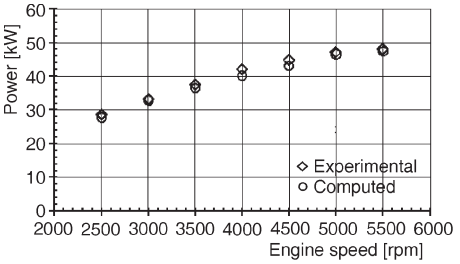

Figure 11. Engine power for CNG fuel

As shown in the figures, in CNG fuel system, torque, and power are less than gasoline. The reduction in power and torque is mainly due to the displacement of some of the air by the fuel gas and the associated reduction in volumetric efficiency because of the absence of the evaporative cooling encountered with liquid fuels applications [44-46]. The relatively lower heating values and slower flame propagation rate of natural gas-air mixture in comparison also contribute to this power loss.

Heat losses

Figures 12 and 13 show the heat losses to the coolent for both fuel types, respectively. The computed results are very close to the experimental data. However, the heat loss in the CNG-fuelled engine is slightly less than that of gasoline-fuelled engine in the operating conditions.

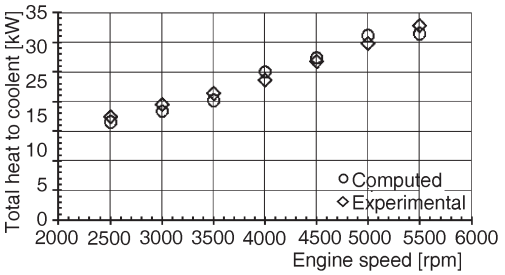

Figure 12. Total heat loss to the coolant for gasoline fuel

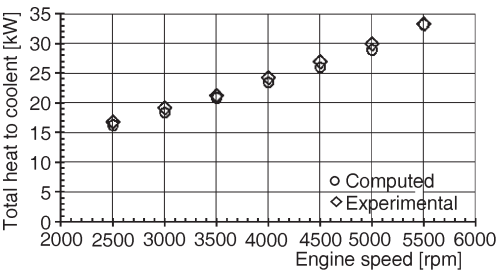

Figure 13. Total heat loss to the coolant for CNG fuel

Conclusions

In this study the existing semi-empirical combustion model has been replaced by a new comprehensive one, which is based on the turbulent flame speed in the combustion chamber. The SI engine performance parameters such as torque, power, and brake specific fuel consumption values for different engine speeds were obtained for both gasoline and CNG fuels. The cylinder working fluid mean temperature, rate of heat fluxes to combustion chamber, and temperature distribution on combustion chamber surfaces were successfully developed in this study. The numerical method to obtain temperature distribution was the alternative direction implicit finite difference method. This method characterized by its implicit nature, unconditional numerical stability and provided an accurate and consistent method for obtaining the temperature distributions. This is done to obtain more realistic and accurate temperature distribution on the surface and inside the SI engines combustion chamber components and also can be used for stress analysis in engine parts or as the proper boundary condition for engine simulation.

The existing three wall heat transfer model has been replaced by a new one. In the new heat transfer model, the combustion chamber has been divided into three zones including cylinder head, cylinder wall, and piston head and heat losses calculated for each part through mean temperature and convective heat transfer coefficient.

The code has been extensively validated with respect to performance and heat transfer against experimental results obtained on XU7JP SI engine with two kinds of fuel (gasoline and CNG) and gave good agreement.

Nomenclature

A – area, [m^2]
A_f – flame front area, [m^2]
D – engine bore, [m]
ff – flame factor, [–]
f_s – geometric coefficient, [–]
h_c – heat transfer coefficient, [Jm^{-2}K^{-1}]
h_e – entrainment enthalpy to control volume, [Jkg^{-1}]
h_i – outgoing enthalpy from control volume, [Jkg^{-1}]
k – thermal conductivity, [Jm^{-1}K^{-1}]
l_i – integral length scale, [m]
l_m – Taylor microscale, [m]
m_e – mass outgoing from control volume, [kg]
m_f – fuel mass entrainment to control volume, [kg]
m_i – mass entrainment to control volume, [kg]
Pr – Prandtl number (= $\nu\alpha^{-1}$), [–]
Q_f – heat release [J]
Q_w – heat transfer to chamber wall, [J]
q_{vs} – fuel heating value, [Jkg^{-1}]
R – gas constant, [Jkg^{-1}K^{-1}]
S_l – laminar flame speed [cms^{-1}]
S_p – piston speed, [rpm]
S_t – turbulent flame speed, [cms^{-1}]
$S_{u,0}$ – flame speed in standard condition, [cms^{-1}]
T_g – gas temperature, [K]
T_u – burned gas temperature [K]
T_w – chamber wall temperature [K]
U – internal energy, [Jkg^{-1}]
u' – turbulence intensity, [ms^{-1}]
W – speed factor, [ms^{-1}]
w – work per cycle, [J]

Greek letters

α – thermal diffusivity, [m^{2}s^{-1}]
ε – turbulent kinetic energy dissipation rate, [m^{3}s^{-2}]
θ – crank angle, [°]
λ – air-fuel ratio, [–]
λ_i – internal equivalence ratio, [–]
ν – kinematic viscosity [m^{2}s^{-1}]
ρ_b – burned gas density, [kgm^{-3}]
ρ_u – unburned gas density, [kgm^{-3}]
ϕ – equivalent ratio, [–]

Acronyms

ADI – alternative direcion implicit
CFD – computational fluid dynamics
CNG – compresed natural gas
ODES – Otto-Diesel-Engine-Simulation
SI – spark ignition

References

[1] Olikara, C., Borman, G., A Computer Program for Calculating Properties of Equilibrium Combustion Products with Some Applications on IC Engines, SAE paper 750468, 1975
[2] Beratta, G. P., Rashidi, M., Keck, J. C., Turbulent Flame Propagation and Combustion in Spark Ignition Engines, *Combust Flame, 52* (1983), pp. 217-245
[3] Kodah, Z. H., *et al*., Combustion in a Spark-Ignition Engine, *Applied Energy, 66* (2000), 3, pp. 237-250
[4] Abd Alla, G. H., Computer Simulation of a Four Stroke Spark Ignition Engine, *Energy Conversion and Management, 43* (2002), 8, pp. 1043-1061
[5] Bayraktar, H., Durgun, O., Development of an Empirical Correlation for Combustion Durations in Spark Ignition Engines, *Energy Conversion Management, 45* (2004), 9-10, pp. 1419-1431
[6] Tomić, M. V., *et al.*, A Quick Simplified Approach to the Evaluation of Combustion Rate from an Internal Combustion Engine Indicator Diagram, *Thermal Science, 12* (2008), 1, pp. 85-102
[7] Tirkey, J. V., Gupta, H. N., Shukla, S. K., Integrated Gas Dynamic and Thermodynamic Computational Modeling of Multicylinder 4- Stroke Spark Ignition Engine Using Gasoline as a Fuel, *Thermal Science, 13* (2009), 3, pp. 113-130
[8] Namazian, M., *et al*., Schlieren Visualization of the Flame and Density Fields in the Cylinder of a Spark-Ignition Engine, SAE paper 800044, 1980, pp. 276-303

[9] Tagalian, J., Heywood, J. B., Flame Initiation in a Spark-Ignition Engine, *Combust Flame, 64* (1986), 2, pp. 243-246
[10] Gatowski, J. A., Heywood, J. B., Deleplace, C., Flame Photographs in a Spark-Ignition Engine, *Combust Flame, 56* (1984), 1, pp.71-81
[11] Thomas, A., Flame Development in Spark-Ignition Engines, *Combust Flame* (1983), 50, pp. 305-322
[12] Lucas, G. G., Brunt, M. F. J., The Effect of Combustion Chamber Shape on the Rate of Combustion in a Spark Ignition Engine, SAE paper 820165, 1982, pp.714-729
[13] Poulos, S. G., Heywood, J. B., The Effect of Chamber Geometry on Spark-Ignition Engine Combustion, SAE paper 830334, 1983, pp. 1106-1129
[14] Basso, A., Optimization of Combustion Chamber Design for Spark Ignition Ignitions, SAE paper 840231, 1984
[15] Hano, R., Isuyoshi, A., Numerical Simulation of Two-Dimensional Combustion Process in a Spark Ignition Engine with a Prechamber Using k-ε Turbulence Model, SAE paper 890669, 1989
[16] Borman, G., Nishiwaki, K., Internal Combustion Engine Heat Transfer, Progress in *Energy and Combustion Science, 13* (1987), 1, pp. 1-46
[17] Yoo, S. J., Kim, E. S., Study of In-Cylinder Local Heat Transfer Characteristic, of a Spark Ignition Engine, SAE paper 931981, 1993, pp. 1-11
[18] Angelberger, C., Poinsot, T., Delhaye, B., Improving Near-Wall Combustion and Wall Heat Transfer Modeling in SI Engines Computations, SAE paper 972881, 1997, pp. 113-130
[19] Urip, E., *et al*., Numerical Investigation of Heat Conduction with Unsteady Thermal Boundary Condition for Internal Combustion Engine Application, *Proceeding on CD*, ASME International Mechanical Engineering Congress, Anaheim, Cal., USA, 2004
[20] Oguri, T., On the Coefficient of Heat Transfer between Gases and Cylinder Walls of the Spark-Ignition Engine, *Bull. JSME,* (1960), 3-11, pp. 363-369
[21] Alkidas, A. C., Heat Transfer Characteristics of a Spark-Ignition Engine, *ASME J. Heat Transfer, 102* (1980), 2, pp. 189-193
[22] Alkidas, A. C., Myers, J. P., Transient Heat-Flux Measurements in the Combustion Chamber of a Spark-Ignition Engine, *ASME J. Heat Transfer, 104* (1982), 1, pp. 62-67
[23] Shayler, P. J., May, S. A., Ma, T., The Determination of Heat Transfer from the Combustion Chambers of SI Engines, SAE paper 931131, 1993
[24] Wallace, F. J., Presentation of Simulation Package ODES at Universally Internal Combustion Engine Group (UNICEG) Meeting, University College London, 1993
[25] Khalilarya, S., An Extended Zero-Dimensional Simulation for HPCR Diesel Engine, Ph. D. thesis, Bath University, Bath, UK, 2002
[26] Wallace, F. J., ODES Data Input Description, Bath University, Bath, UK, 1993
[27] Bayraktar, H., Durgun, O., Mathematical Modeling of Spark-Ignition Engine Cycles, *Energy Sour., 7* (2003), 25, pp. 651-66
[28] Kreiger, R. B., Borman, G. L., The Computation of Apparent Heat Release for Internal Combustion Engines, ASME paper 66-WAI/GP-4, 1966
[29] Taylor, C. F., The Internal Combustion Engine in Theory and Practice, vol. 2, MIT Press, Cambridge, Mass., USA, 1968
[30] Heywood, J. B., Internal Combustion Engine Fundamentals, McGraw-Hill, New York, USA, 1988
[31] Nusselt, W., Heat Transfer in Internal Combustion Engines (in German), *Ingenieur, 67* (1923), pp. 692-708
[32] Annand, W. J. D., Heat Transfer in the Cylinders of Reciprocating Internal Combustion Engines, Proceedings of the Institution of Mechanical Engineers, 1963, No. 177-36, pp. 973-990
[33] Eichelberg, G., Some New Investigations on Old Combustion Engine Problems, *Engineering* (1939), 148, pp. 463-547
[34] Woschni, G., A University Applicable Equation for Instantaneous Heat Transfer Coefficient in Internal Combustion Engines, SAE paper 670931, *SAE Trans, Vol. 76* (1976)
[35] Benson, R. S., Horlock, J. H., Winterbone, D. E., The Thermodynamics and Gas Dynamics of Internal Combustion Engines, vol. 1, Clarendon Press, Oxford, UK, 1982
[36] Blizard, N. C., Keck, J. C., Experimental and Theoretical Investigation of Turbulent Burning Model for Internal Combustion Engines, SAE paper 740191, *SAE Trans., Vol. 83* (1974)

[37] Tabaczynski, R. J., Ferguson, C.R., Ranha Krishnan, K., A Turbulent Entrainment Model for Spark Ignition Engine Combustion, SAE paper 770647, *SAE Trans., Vol. 86* (1977)
[38] Polous, S. G., Heywood, J. B., The Effect of Chamber Geometry on Spark-Ignition Engine Combustion, SAE paper 830334, 1983
[39] Tennekes, H., Lumley, J. L., A First Course in Turbulence, MIT Press, Cambridge, Mass., USA, 1972
[40] Heywood, J. B., Internal Combustion Engine Fundamentals, McGraw-Hill, New York, USA, 1988
[41] Hoffmann, K. A., Chain, S. T., Computational Fluid Dynamics for Engineers, McGraw-Hill, New York, USA, 1995
[42] Churchill, S. W., Bernstein, M., A Correlation Equation for Forced Convection from Gases and Liquids to a Circular Cylinder in Cross Flow, *J. Heat Transfer, 99* (1977), 2, pp.300-306
[43] ***, Iranian Power Training Company (IPCO), http://www.ip-co.com/
[44] Tennant, C. J., *et al*., Turbocharging a Bi-Fuel Engine for Performance Equivalent to Gasoline, SAE paper 942003, 1994
[45] Hyun, C. C., *et al*., Development Work on HMC's Natural Gas-Fueled 1.5 L MPI DOHC Engine, SAE paper 931869, 1993
[46] Ishii, M., *et al*., Experimental Studies on a Natural Gas Vehicles, SAE paper 942005, 1994

Paper submitted: March 16, 2010
Paper revised: May 25, 2010
Paper accepted: October 19, 2010